ChemComm

Accepted Manuscript

This article can be cited before page numbers have been issued, to do this please use: H. Mai, Y. Wang, S. Li, R. Jia, S. Li, Q. Peng, Y. Xie, X. hu and S. Wu, *Chem. Commun.*, 2019, DOI: 10.1039/C9CC02289A.

ROYAL SOCIETY OF CHEMISTRY

rsc.li/chemcomm

ROYAL SOCIETY OF CHEMISTRY View Article Online
DOI: 10.1039/C9CC02289A

Journal Name

COMMUNICATION

A pH-sensitive near-infrared fluorescent probe with alkaline pKa for chronic wounds monitoring in diabetic mice

Received 00th January 20xx,
Accepted 00th January 20xx

DOI: 10.1039/x0xx00000x

www.rsc.org/

Hengtang Mai,[a] Yu Wang ,[b] Shuang Li,[a] Ruizhen Jia,[a] Sixian Li,[a] Qian Peng,[a] Yan Xie,[a] Xiang Hu[b] and Song Wu* [a]

A pH-sensitive near-infrared fluorescent probe with alkaline pKa, AlkaP-1, was developed by incorporating a benzoyl hydrazine group into a cyanine dye. The significant fluorescence changes in the alkaline regions enable the probe to monitor the alkalization process from acute wounds to chronic wounds in diabetic mice.

In complex bioorganisms like human being, pH environments vary vastly from strong acidic gastric fluid to basic pancreatic secretion, which are vital to perform normal physiological functions.[1] Abnormalities of pH environments in biosystems are usually indicators of occurrence of diseases, such as in the case of development of chronic wounds.[2] Chronic wounds become caught in a state of inflammation, making higher levels of degrading proteases, which alter components of the extracellular matrix that are vital to the wound healing process. pH plays a significant role in affecting cellular processes in the wound, which in turn affects the healing process.[3] Skin surface on a health human is slight acidic (4.2-5.9),[4] but neutralized by body fluid leakage when the underlying tissue wounded (acute wound), and more alkaline (7.14-8.9) at the stage of chronic wound if delayed healing happened under certain pathological circumstances.[5] Many types of chronic wounds, including venous leg ulcer, diabetic foot ulcer and bedsore, not only seriously affect the quality of life of the patients, but also bring about a heavy financial burden.[6] It is reported that the cost of the treatment of chronic wounds accounts for one-third of the dermatological health budget in the United States. Monitoring the wound pH may provide a tool to determine the condition of the wound bed and help to optimize the clinical therapeutic schedule.[7] So far the reported tools for pH measurement for chronic wounds Include glass electrode, electrochemical method, and luminescent probes, suffering from either only single-spot value detectable, or on-spot, and real time detection inapplicable.[8] There is a great demand for the development of straightforward tools with high spatio-temporal resolutions.

Near-infrared (NIR) fluorescence imaging of biological parameters is a burgeoning area in biomedical sciences. It is well-known that NIR emission from 650 to 900 nm has the biological merits of less photodamage, deep tissue penetration, and less autofluorescence interference created by biomolecules in the living system.[9] Many types of pH-sensitive NIR fluorescence probes have been developed, for the various purposes from diagnosis of tumors[10] to measurements of small changes in living cells and organells.[11] However, most of these probes function in acidic regions with pKa less than 7.5, which are unsuitable for monitoring pH changes in alkaline chronic wounds. Therefore, it is very important to develop NIR fluorescent probes with an appropriate alkaline pKa for practical bioimaging applications on the chronic wounds.

Herein we report our efforts on the development of **AlkaP-1,** a new pH-sensitive NIR fluorescence probe, which is obtained by rational design (Scheme 1). For the first time, **AlkaP-1** is successfully employed to visualize alkalization in the course of chronic wound development from acute wound in a transgenetic diabetic mouse model due to its unique optical characteristics toward pH.

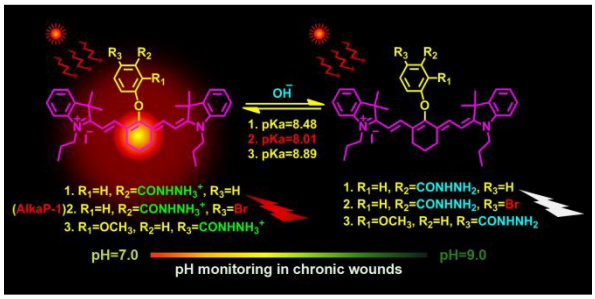

Scheme 1 Chemical structures of the NIR fluorescent compounds (**1, 2** and **3**) and their structural responses to pH changes.

[a] Hubei Province Engineering and Technology Research Center for Fluorinated Pharmaceuticals, School of Pharmaceutical Sciences, Wuhan University, Wuhan, Hubei, 430072, P. R. China.
[b] Department of Orthopaedic Trauma and Microsurgy, Zhongnan Hospital of Wuhan University, Wuhan, Hubei, 430071, China.

†Electronic Supplementary Information (ESI) available: Experimental section, HRMS and NMR, optical spectra, determination of pKa, stability and selectivity experiment, cytotoxicity assay, live cell imaging, and animal experiments. See DOI: 10.1039/x0xx00000x

Given the pH environments in chronic wounds, we consider that an ideal pH-sensitive NIR fluorescence probe for these diseases requires showing significant fluorescent changes among narrow pH ranges (ca. 7.0-9.0). The key point to design a pH-sensitive probe relies on the protonization/deprotonization of a reactive moiety attached to a NIR fluorophore based on the photoinduced electron transfer (PET) mechanism. The reported reactive moieties, including morpholinyl group[12], piperazinyl group[13], indolyl group[14], anilino group[10a,10b,11a], , etc,[11b,11c] have been utilized to construct probes responsive to acidic pH due to their relative low pKa values. We postulated that acylhydrazine compounds, which are reported to possess higher pKa,[15] may act as reactive moieties of the probes that are responsive to alkaline pH conditions for chronic wounds. For the proof-of-concept test, we initially designed compound **1** containing a benzoyl hydrazine cationic group, which can enhance the water-solubility of the probe, attached to a widely used NIR fluorophore Cy7[16] via an ether linker. Using 3-hydroxybenzoate as the starting material, we synthesized the intermediate tert-butyl 2-(3-hydroxybenzoyl) hydrazine carboxylate (**1b**) via a two-step reaction including hydrazinolysis by hydrazine and protection of acylhydarzine group by N-tert-butoxycarbonylation (Boc). The next condensation between **1b** and CyCl (IR-780) under basic conditions gave the precursor **1c**, followed by the deprotection of Boc group to offer the desired green compound **1** (Scheme S1, ESI†). Compound **1** was fully characterized by NMR and HRMS.

The optical response of compound **1** toward pH was then studied in citrate-phosphate and carbonate-bicarbonate buffers, respectively. As shown in Fig. 1a, the absorption peaks around 770 nm gradually decreased with the increasing pH among 4.5-10.5. Interestingly, the fluorescence spectra as shown in Fig. 1b exhibited a quite different variation tendency. At acidic regions among 4.5 to 7.0, the fluorescence displayed weak changes, while sharply dropped among the alkaline pH region. The decreasing of fluorescence may ascribed to the PET effect, namely, the cationic compound **1** turns to its nonfluorescent non-protonated form with pH increasing. The pka of compound **1**, was calculated to be 8.48 (Fig. S2a, ESI†). The above consequences proved our hypothesis that introduction of acylhydrazine to the fluorophore makes major fluorescence changes in alkaline regions. But unfortunately, at the pH region of 7.0-9.0 that we are interested, only an intermediate fluorescence intensity change about 2.6-fold was observed, which is not good enough for the chronic wounds pH monitoring.

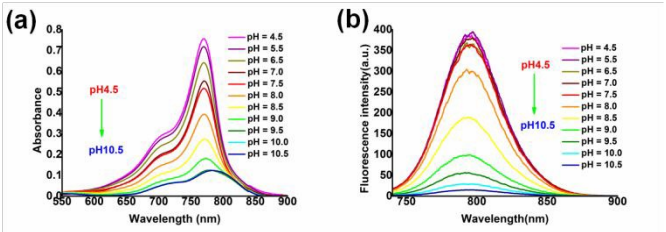

Fig. 1 (a) Absorbance spectra of 5 μM compound **1** with different pH buffers containing 10 % DMSO. (b)Fluorescence spectra of 10 μM compound **1** with different pH buffers containing 10 % DMSO at excitation of 715 nm.

Next, we sought to tune the optical performance of the fluorescent compounds containing acylhydrazine by structural modification, using **1** as a lead compound. Introduction of an electron-withdrawing group to benzene ring may reduce the electron density of the terminal amino group and make the amino group less alkaline, by which pKa may be reduced. Based on the above analysis, we designed compound **2** by introduction of bromine atom adjacent to the acylhydrazine group. Meanwhile, to prove the effect of different substituents on optical performance, compound **3**, an analogue of compound **1**, with an electron-donating methoxy group, was also designed. Compound **2** and **3** were synthesized via a similar synthetic route to compound **1** and characterized (Scheme S1, ESI †). Their optical performances to pH were evaluated (Fig. S1, ESI †). The overall absorbance and fluorescence responsive tendencies of the both compounds toward pH are similar to that of compound **1**. But at alkaline regions from 7.0-9.0, the fluorescence change ratios for compound **2** and **3** are 10.0 and 0.6-fold, respectively. The pkas of compound **2** and **3**, were calculated to be 8.01 and 8.89, respectively (Fig. S2b-c, ESI†). Apparently, substituents with different electronic effects can alter the pKa values, leading to the different optical performances to pH. Among the pH range from 7.0 to 9.0, the higher pka of the compound corresponds to the weaker fluorescence changes. Considering that compound **2** has largest fluorescence changes among 7.0-9.0, it was selected for the further bioimaging studies and named as **AlkaP-1**. The quantum yield of **AlkaP-1**, was measured to be 4.2% at pH 4.5 and 0.6% at pH 9.5, respective ly, suggesting the great environmental impact on the optical properties of the probe (Fig. S3, ESI†).

We investigated the photostability of **AlkaP-1** at acidic and alkaline conditions, respectively, by irradiating them at 715 nm and measuring fluorescence intensity at different time points (Fig. S4, ESI†). At pH 4.5, the fluorescence intensity of **AlkaP-1** showed only a maximum decrease by 14.5% after 1 h irradiation, while an even lower decrease ratio of 7.0% could be observed at pH 9.5, indicating the good photostability of the probe under the both conditions. Meanwhile, the selectivity of **AlkaP-1** to pH in the presence of a variety of metal ions, anions, biothiols, and amino acids was investigated by fluorescence spectra at pH 4.5, 7.5, and 10.0, respectively (Fig. S5, ESI †). All the biologically relevant species exhibited little influences on fluorescence intensities, suggesting the good selectivity of the probe.

A standard cell viability protocol (MTT assay) was employed to study the cytotoxicity of the probe on Ewing's Sarcoma cells A673 by treating cells with various concentrations of **AlkaP-1** (5, 10, 20 μM) for 24 h (Fig. S6, ESI †). **AlkaP-1** showed low cytotoxicity and good compatibility with over 80% cell viability at the highest concentration of 20 μM. We further determined the optimal intracellular working concentration of **AlkaP-1**. The fluorescence imaging in living cells was conducted by incubating Ewing's Sarcoma cells A673 with 5, 10, 15, and 20 μM **AlkaP-1** in PBS, respectively. The fluorescence intensity in

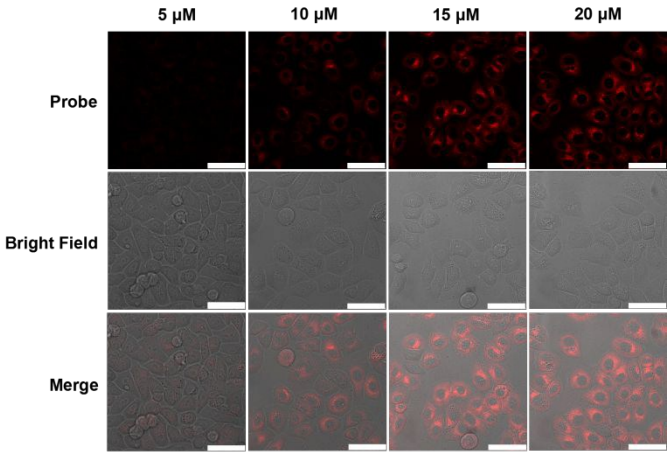

Fig. 2 Fluorescence images of Ewing's Sarcoma cells incubated with 5, 10, 15, and 20 μM **AlkaP-1** in PBS, respectively. Images were taken using the confocal fluorescence microscope at 60 × magnification, scale bars = 50 μm.

cells increased with concentration of the probe, and reached its maximum at 15 μM (Fig. 2), while the higher concentration at 20 μM did not offer significant fluorescence increasing. We thus chose the concentration of 15 μM for the next studies based on the optical performance and cytotocixity evaluation in cells.

In order to investigate whether the AlkaP-1 could be used to reflect pH changes in living cells, the fluorescence imaging of live cells with different intracellular pH values was conducted by incubating Ewing's Sarcoma cells A673 with 15 μM **AlkaP-1**, and then with nigericin (15 μg/mL) (H^+/K^+ ionophore) in buffers with different pH values at 4.5, 7.0, 7.5, 8.0, 8.5, 9.0, 9.5, respectively, where nigericin was used to equilibrate the intracellular and extracellular pHs.[13] As shown in Fig. 3, the cellular fluorescence irregularly decreased with the increasing pH. In the acidic region from 4.5 to 7.0, only a low fluorescence change about 8.4% was observed, while it dropped about 76.9% in the alkaline regions from 7.0 to 9.0. This tendency is coincident with that observed in vitro. Apparently, **AlkaP-1** could indeed detect the pH changes particularly the alkaline regions in living cells.

The development of chronic wounds, especially in diabetic ulcers, usually accompanies with an increase of the alkalinity due to wound infections, which therefore result in delayed wound healing.[17] A transgenetic diabetes-impaired *db/db* mouse model has been used for studies of chronic wound healing in diabetic foot ulcers.[18] To study the pH changes during chronic wounds development, we created six excisional wounds, roughly in two parallel lines on the back of one *db/db* mouse. These excisional wounds are reliable to form chronic wounds that are hard to heal. **AlkaP-1** was then sprayed into the each wound bed on the right side at 1, 4, and 7 days, respectively, after the excision. Meanwhile, the wounds on the left side keep intact for comparison. As shown in Fig. 4, the bright fluorescence could be observed at the stage of acute wound (day 1), but gradually decreased as the time went on, reflecting that pH of the wound bed is increasing. Semiquantitative analysis to fluorescence intensity of each wound by employing imaging system analysis software showed about 45% of decreased fluorescence from day 1 to day 7 (Fig S7a, ESI †). Meanwhile, the average surface pH changes of the wound bed measured by a flat glass pH electrode[19] showed increase from 6.97 to 8.06 within 7 days (Fig S7b, ESI †). Both approaches reflect the alkalization processes during the development of chronic wounds. In addition, we also noticed that the pH distribution of every wound is uneven (Fig. 4a-c), which may be useful to visualize the heterogeneity of pH within the wound bed during the different developmental stages of chronic wounds. The above observations, not only prove the alkalization processes occur during the course of the delayed healing of chronic wounds, but also provide the detailed information of the pH distributions in the whole wound area.

In summary, we developed a pH-sensitive NIR fluorescent probe, **AlkaP-1**, based on benzoyl hydrazine structure by rational design. The characteristic responses to pH in the

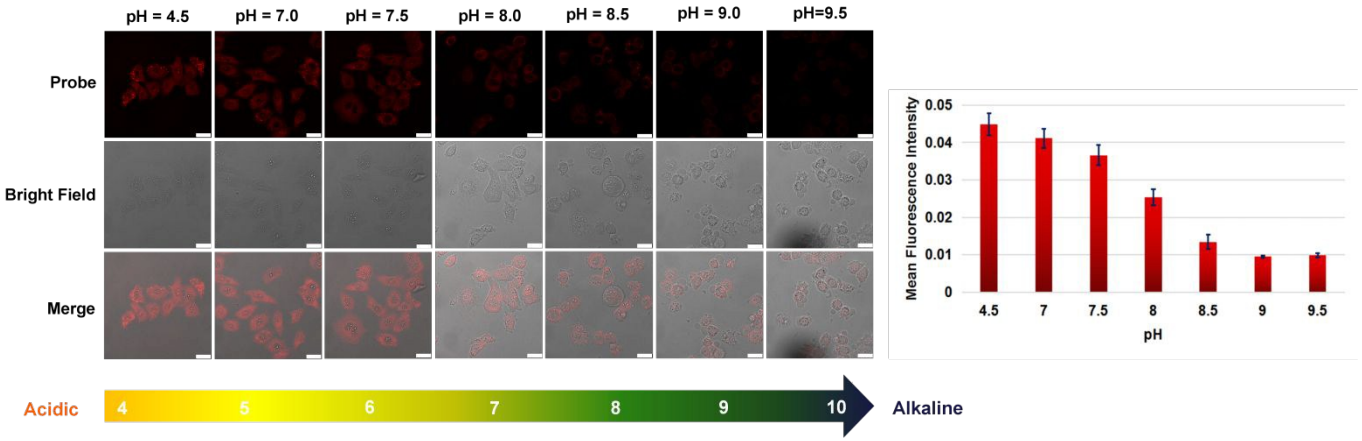

Fig. 3 Fluorescence images of Ewing 's Sarcoma cells incubated with 15 μM **AlkaP-1** for 30 min in buffers with different pH values of 4.5, 7.0, 7.5, 8.0, 8.5, 9.0 and 9.5 containing 15 μg/mL nigericin. Images were collected using a confocal fluorescence microscope magnification, scale bars = 25 μM. Quantified relative fluorescence intensity of a certain pH was obtained employing Image-Pro Plus software and presented as mean ± SD, with n = 3.

View Article Online
DOI: 10.1039/C9CC02289A

Journal Name

COMMUNICATION

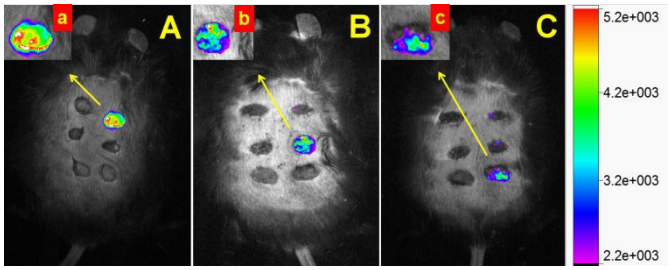

Fig. 4 The fluorescence intensity within the wound beds at different time points are recorded by the pseudocolor images **A** (day 1), **B** (day 4), **C** (day 7), respectively. **a**, **b**, and **c** are the partially enlarged views of the pseudocolor images A, B, and C, respectively.

alkaline regions render **AlkaP-1** ability to visualize the pH changes in the course of chronic wounds development in living system. In addition, the uneven pH distribution of wound disclosed by the probe, suggests that we may correlate the pH with the heterogeneous morphology of wounds. Our probe provides a potential tool to evaluate the condition of the wound bed, which will benefit the treatment of the related diseases.

This research reported in this publication was supported by the National Natural Science Foundation of China (Grant No. 21572174)

Conflicts of interest

There are no conflicts to declare.

Notes and references

1 (a) D. Schmaljohann, *Adv. Drug Delivery Rev.*, 2006, **58**, 1655-1670; (b) J. R. Casey, S. Grinstein and J. Orlowski, Nat. Rev. *Mol cell Biol*., 2010, **11**, 50-61; (c) D. M. Lynn, M. M. Amiji and R. Langer, *Angew. Chem.*, 2001, **113**, 1757-1760.
2 (a) J. Posnett, P. J. Franks, *NT*, 2008, **104**, 44-45; (b) J. G. Powers, *J. Am. Acad. Dermatol*., 2016, **74**, 607-625.
3 E. M. Jones, C. A. Cochrane and S. L. Percival, *Adv. Wound Care*, 2015, **4**, 431-439.
4 (a) H. C. Korting and O. Braun, *Clin. Dermatol.*, 1995, **14**, 23-27; (b) C. Ehlers, U. I. Ivens, M. L. Møller, T. Senderovitz and J. Serup, *Skin Res. Technol.*, 2001, **7**, 90-94.
5 G. Gethin, *Wounds UK*, 2007, **3**, 52-56;
6 G. A. James, E. Swogger, R. Wolcott, E. D. Pulcini, P. Secor, J. Sestrich, J. W. Costerton, P. S. Stewart, *Wound Rep. Reg*., 2008, **16**, 37-44.
7 (a) R. E. Jones, D. S. Foster and M. T. Longaker, *JAMA*, 2018, **320**, 1481-1482; (b) M. L. Goff, B. Mourgeon, J. Blanchère, L. Teot, H. Benateau and A. Dompmartin, *Int. J. Technol. Assess Health Care*, 2018, **34**, 567-575; (c) D. Chicharro, M. Rubio, E. Damiá, J. M. Carrillo, B. Cuervo, P. Peláez and J. J. Sopena, *J. Funct. Biomater*. 2018, **9**, 1-20.
8 (a) S. Schremla, R. J. Meierb, O. S. Wolfbeisb, M. Landthalera, R. Szeimiesa and P. Babilas, *PNAS*, 2011, **108**, 2432-2437; (b) T. R. Dargaville, B. L. Farrugia, J. A. Broadbent, S. Pace, Zee Upton and N. H. Voelcker, *Biosens. Bioelectron.*, 2013, **41**, 30-42; (c) D. Sharp, *Biosens. Bioelectron.*, 2013, **50**, 399-405.
9 (a) R. Weissleder, *Nat. Biotechnol*. 2001, **19**, 316-317; (b) F. Yu, X. Han and L. Chen, *Chem. Commun.*, 2014, **50**, 12234-12249; (c) D. Ye, A. J. Shuhendler, L. Cui, L. Tong, S. S. Tee, G. Tikhomirov, D. W. Felsher and J. Rao, *Nat. Chem.*, 2014, **6**, 519-526.
10 (a) C. Tung, J. J. Qi, L. C. Hu, M. S. Han and Y. Kim, *Theranostics*, 2015, **5**, 1166-1174; (b) J. Y. Zhang, Z. N. Liu, P. Lian, J. Qian and X.W. Li, *Chem. Sci*., 2016, **7**, 5995-6005; (c) X. D. Liu, Q. Chen, G. B. Yang, L. F. Zhang, Z. Liu, Z. P. Cheng and X. L. Zhu, *J. Mater. Chem. B*, 2015, **3**, 2786-2800.
11 (a) P. Li, H. B. Xiao, Y. F. Cheng, W. Zhang, F. Huang, W. Zhang, H. Wang and B. Tang, *Chem. Commun*., 2014, **50**, 7184-7187; (b) Y. H. Li, Y. J. Wang, S. Yang, Y. R. Zhao, L. Yuan, J. Zheng and R. H. Yang, *Anal. Chem*., 2015, **87**, 2495-2503; (c) Y. Zhang, S. Xia, M.X. Fang, W. Mazi, Y. B. Zeng,T. Johnston, A. Pap, R. L. Luck and H. Y. Liu, *Chem. Commun.*, 2018, **54**, 7625-7628.
12 (a) J. Zhang, M. Yang, W. Mazi, K. Adhikari, M. Fang, F. Xie, L. Valenzano, A. Tiwari, F. Luo and H. Liu, *ACS Sens.*, 2016, **1**, 158-165.; (b) P. Ning, L. Hou, Y. Feng, G. Xu, Y. Bai, H. Yua and X. Meng, *Chem. Commun*., 2019, **55**, 1782-1785.
13 J. Zhang, M. Yang, C. Li, N. Dorh, F. Xie, F. Luo, A. Tiwari and H. Liu, *J. Mater. Chem. B*, 2015, **3**, 2173-2184.
14 (a) L. Fan, Y. Fu, Q. Liu, D. Lu, C. Dong and S. Shuang, *Chem. Commun.*, 2012, **48**, 11202-11204.; (b) X. Liu, Y. Xu, R. Sun, Y. Xu, J. Lu and J. Ge, *Analyst,* 2013, **138**, 6542-6550.
15 F. Milletti, L. Storchi, L. Goracci, S. Bendels, B. Wagner, M. Kansy and G. Cruciani, *Eur. J. Med. Chem.*, 2010, **45**, 4270-4279.
16 M. X. Fang, S. Xia, J. H. Bi, T. P. Wigstrom, L. Valenzano, J. B. Wang, W. F. Mazi, M. Tanasova, F. T. Luo and H. Y. Liu, *Chem. Commun*., 2018, **54**, 1133-1136.
17 (a) H. H. Leveen, G. Falk, B. Borek, C. Diaz, Y. Lynfield, B. J. Wynkoop, G. A. Mabunda, J. L. Rubricius and G. C. Christoudias, *Ann. Surg*., 1973, **178**, 745-753; (b) S. Ono, R. Imai, Y. Ida, D. Shibata, T. Komiya and H. Matsumura, *burns*, 2015, **41**, 820-824; (c) C. McArdle, K. M. Lagan and D. A. McDowell, *Curr. Diabetes Rev*., 2014, **10**, 177-181.
18 (a) Y. Kitano, K. Yoshimura, G. Uchida, K. Sato and K. Harii, *Arch Dermatol Res*., 2001, **293**, 515-521; (b) P. Y. Lee, S. Chesnoy, and L. Huang, *J. Invest Dermatol.*, 2004, **123**, 791-798.
19 (a) M.-H. Schmid-Wendtnera and H.C. Korting, *Skin Pharmacol. Physiol.*, 2006, **19**, 296-302. (b) S. Dikstein and A. Zlotogorski, *Acta Derm. Venereol. (Stockh)*, 1994, **185**, 18-20.

View Article Online
DOI: 10.1039/C9CC02289A

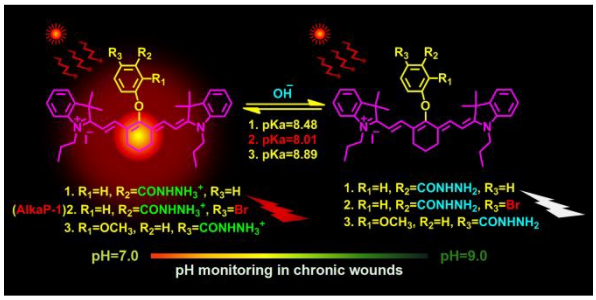

An alkaline pH-sensitive near-infrared fluorescence probe can monitor pH changes in the course of chronic wounds developments in mice.